Reproducibility of Complex Turbulent Flow Using Commercially-Available CFD Software

—Report 2: For the Case of a Two-Dimensional Ridge With Steep Slopes—

Takanori UCHIDA*1

E-mail of corresponding author: *takanori@riam.kyushu-u.ac.jp*

(Received January 29, 2016)

Abstract

Choosing appropriate sites for wind turbines is extremely important in Japan because the spatial distribution of wind speed is highly complex over steep complex terrain, which is abundant in Japan. The author's research group has been developing an unsteady CFD software package called RIAM-COMPACT®. This package is based on an LES turbulence model. In this paper, to examine the accuracy of RIAM-COMPACT®, numerical simulations of uniform, non-stratified airflow over a two-dimensional ridge were performed. The analysis primarily focused on airflow characteristics in the wake region. The results from the simulation with RIAM-COMPACT® were compared to those from a commercially-available CFD software package (STAR-CCM+), and no significant differences were found among these results.

Key words: *Commercially-available CFD software, STAR-CCM+, RIAM-COMPACT®, Ridge model*

1. Introduction

The author's research group has developed the numerical wind diagnosis technique named RIAM-COMPACT® [1, 2]. The core technology of RIAM-COMPACT® is under continuous development at the Research Institute for Applied Mechanics, Kyushu University, Japan. An exclusive license of the core technology has been granted by Kyushu TLO Co., Ltd. (Kyushu University TLO) to RIAM-COMPACT Co., Ltd. (http://www.riam-compact.com/), a venture corporation which was founded by the author and originated at Kyushu University in 2006. A trademark, RIAM-COMPACT®, and a utility model patent were granted to RIAM-COMPACT Co., Ltd. in the same year. In the meantime, a software package has been developed based on the above-mentioned technique and is named the RIAM-COMPACT® natural terrain version software. Efforts have been made to promote this software as a standard software package in the wind power industry.

In the previous paper[2], a numerical simulation was performed for airflow around an isolated-hill with a steep slope angle using RIAM-COMPACT® natural terrain version, and the results were compared to those from numerical simulations performed using another commercially-available CFD software package. In the present paper, a similar study is conducted for airflow over a ridge, the shape of which is identical to the shape created by extending the central cross-section of the isolated-hill from the previous paper[2] continuously in the spanwise (y) direction. The results of the comparisons are discussed.

2. Summary of Commercially-Available CFD Software

Commercially-available computational fluid dynamics (CFD) software packages have been developed and used mainly as design tools primarily in the automobile and aviation industries up to the present time. The following is a list of the major CFD software packages available on the market:

General-purpose CFD thermal fluid analysis software packages

■STAR-CCM+
http://www.cd-adapco.co.jp/products/star_ccm_plus/index.html

■ANSYS(CFD, Fluent, CFX)
http://ansys.jp/solutions/analysis/fluid/index.html

■SCRYU/Tetra
http://www.cradle.co.jp/products/scryutetra/

■STREAM
http://www.cradle.co.jp/products/stream/index.html

■CFD2000
http://www.cae-sc.jp/docs/cfd2000/index.htm

■PHOENICS
http://www.phoenics.co.jp/

*1 Research Institute for Applied Mechanics, Kyushu University

■Autodesk Simulation CFD
http://www.cfdesign.com/

■CFD++
http://bakuhatsu.jp/software/cfd/

■CFD-ACE+
http://www.wavefront.co.jp/CAE/cfd-ace-plus/

■AcuSolve
http://acusolve.jsol.co.jp/index.html

■FLOW-3D
http://www.terrabyte.co.jp/FLOW-3D/flow3d.htm

■FloEFD
http://www.sbd.jp/product/netsu/floefd3cad.shtml

■Flow Designer
http://www.akl.co.jp/

■PowerFLOW
http://www.exajapan.jp/pages/products/pflow_main.html

■KeyFlow
http://www.kagiken.co.jp/product/keyflow/index.shtml

■OpenFOAM
http://www.cae-sc.jp/docs/FOAM/

■FrontFlow
http://www.advancesoft.jp/product/advance_frontflow_red/

The wind power industry has independently developed and distributed CFD software designed for selecting sites appropriate for the installation of wind turbines (see the list below). Recently, some of the above-listed general-purpose thermal fluid analysis software packages have also started being adopted in the wind power industry.

CFD software packages designed for the wind power industry (wind farm design tools)

■RIAM-COMPACT®
http://www.riam-compact.com/

■MASCOT
http://aquanet21.ddo.jp/mascot/

■WindSim
http://www.windsim.com/

■METEODYN
http://meteodyn.com/

In the present paper, the simulation results from RIAM-COMPACT® natural terrain version are compared to those from STAR-CCM+, one of the leading commercially-available CFD software packages. The results of the comparison are discussed.

3. Summary of STAR-CCM+ Software

In this section, a summary of STAR-CCM+, a general-purpose thermal fluid analysis software package distributed by CD-adapco is provided (see Table 1). The version of the software package used in the present study is 8.02.008 (for 64-bit Windows).

STAR-CCM+ uses a single graphical user interface (GUI) for computational grid generation, execution of fluid analyses, and data post-processing. The grid generation method in STAR-CCM+ is distinctive. In STAR-CCM+, both a polyhedral grid and a prism layer grid can be used (for example, see Fig.3). The polyhedral grid is a new type of grid offered and promoted by CD-adapco and consists of polyhedral cells which possess 10 to 15 faces on average. The use of this cell type makes it possible to dramatically reduce 1) the number of grid cells required to obtain analysis results equivalent to those that can be obtained using a conventional tetrahedral grid and 2) the memory required by the solver. With the use of this cell type, the computational stability improves significantly, and the time required to obtain convergent solutions also decreases. The prism layer grid is a refined grid designed to capture the behavior of the boundary layer that develops over the surface of an object. In this type of grid, layers of thin grid cells are distributed regularly over the object. Since the thickness and number of layers in the normal direction with respect to the object surface can be freely adjusted, the behavior of the boundary layer in the vicinity of a wall can be captured with high accuracy. However, when the number of prism layer grid cells is very large, the computation time increases significantly.

Numerical simulations are based on the finite-volume method (FVM), and the Navier-Stokes equation is used as the governing equation. Iterative calculations are performed for the velocity and pressure fields using an algebraic multi-grid (AMG) linear solver. For the time marching method, a first-order implicit method is used. STAR-CCM+ can be run either with a Reynolds-averaged Navier-Stokes (RANS) turbulence model or a large-eddy simulation (LES) turbulence model. For the convective term in the RANS models, a second-order upwind scheme is adopted. For the convective term in the LES models, a bounded central differencing (BCD) scheme is employed. Table 1 shows an overview of the computational techniques,

parameters, and simulation set-up used for one of the simulations performed with STAR-CCM+ in the present study, namely the simulation with a steady RANS turbulence model, as an example.

Simulation code	**STAR-CCM+ v.8.02.008**
Governing equation	Three-dimensional unsteady Navier-Stokes equation
Turbulence model	Steady RANS (Spalart-Allmaras one-equation eddy-viscosity turbulence model)
Time marching	1. First-order implicit unsteady analysis 2. Steady analysis (The steady-state solution is obtained by specifying the number of time steps.)
Duration of simulation	1. Spin-up: 0 – 100s in non-dimensional time (Time averaging: 100 – 200s in non-dimensional time) 2. Spin-up: 0 – 2000 in time step number (Time averaging: 2000 - 4000 in time step number)
Discretization of the convective term	A second-order upwind scheme (No options available other than first-order and second-order upwind schemes)
Gas	Constant density
Density ρ	1.0 [kg/m^3]
Coefficient of viscosity μ	1.0×10^{-5} [Pa•s]
Ridge model height h	0.1 [m]
Inflow wind velocity U	1.0 [m/s]
Reynolds number $= U\,h\,(\rho / \mu) = U\,h / \nu$	1.0×10^4
Non-dimensional time step $\Delta t = (\Delta t\,U) / h$	2.5×10^{-2}
Number of grid cells	Approx. 1.5 million

Table 1 Overview of STAR-CCM+, for the case of the simulation using a steady RANS model in the present study

4. Summary of RIAM-COMPACT® Software

In this section, a summary of RIAM-COMPACT® natural terrain version, developed by the author's research group, will be described. In this software package, a collocated grid in a general curvilinear coordinate system is adopted in order to numerically predict local wind flow over complex terrain with high accuracy while avoiding numerical instability. In this collocated grid, the velocity components and pressure are defined at the grid cell centers, and variables that result from multiplying the contravariant velocity components by the Jacobian are defined at the cell faces. The numerical technique is based on the finite-difference method (FDM), and an LES model is adopted for the turbulence model. In LES models, a spatial filter is applied to the flow field to separate eddies of various scales into grid-scale (GS) components, which are larger than the computational grid cells, and sub-grid scale (SGS) components, which are smaller than the computational grid cells. Large-scale eddies, i.e., the GS components of turbulence eddies, are directly numerically simulated without the use of a physically simplified model. In contrast, dissipation of energy, which is the main effect of small-scale eddies, i.e., the SGS components, is modeled according to a physics-based analysis of the SGS stress.

For the governing equations of the flow, a spatially-filtered continuity equation for incompressible fluid (Eq.(1)) and a spatially-filtered Navier-Stokes equation (Eq.(2)) are used.

$$\frac{\partial \bar{u}_i}{\partial x_i} = 0 \qquad \text{-(1)}$$

$$\frac{\partial \bar{u}_i}{\partial t} + \bar{u}_j \frac{\partial \bar{u}_i}{\partial x_j} = -\frac{\partial \bar{p}}{\partial x_i} + \frac{1}{Re}\frac{\partial^2 \bar{u}_i}{\partial x_j \partial x_j} - \frac{\partial \tau_{ij}}{\partial x_j} \qquad \text{-(2)}$$

$$\tau_{ij} \approx \overline{u_i' u_j'} \approx \frac{1}{3}\overline{u_k' u_k'}\delta_{ij} - 2\nu_{SGS}\bar{S}_{ij} \qquad \text{-(3)}$$

$$\nu_{SGS} = \left(C_s f_s \Delta\right)^2 \left|\bar{S}\right| \qquad \text{-(4)}$$

$$\left|\bar{S}\right| = \left(2\bar{S}_{ij}\bar{S}_{ij}\right)^{1/2} \qquad \text{-(5)}$$

$$\bar{S}_{ij} = \frac{1}{2}\left(\frac{\partial \bar{u}_i}{\partial x_j} + \frac{\partial \bar{u}_j}{\partial x_i}\right) \qquad \text{-(6)}$$

$$f_s = 1 - \exp\left(-z^+ / 25\right) \qquad \text{-(7)}$$

$$\Delta = \left(h_x h_y h_z\right)^{1/3} \qquad \text{-(8)}$$

For the computational algorithm, a method similar to a fractional step (FS) method is used, and a time marching method based on the Euler explicit method is adopted. The

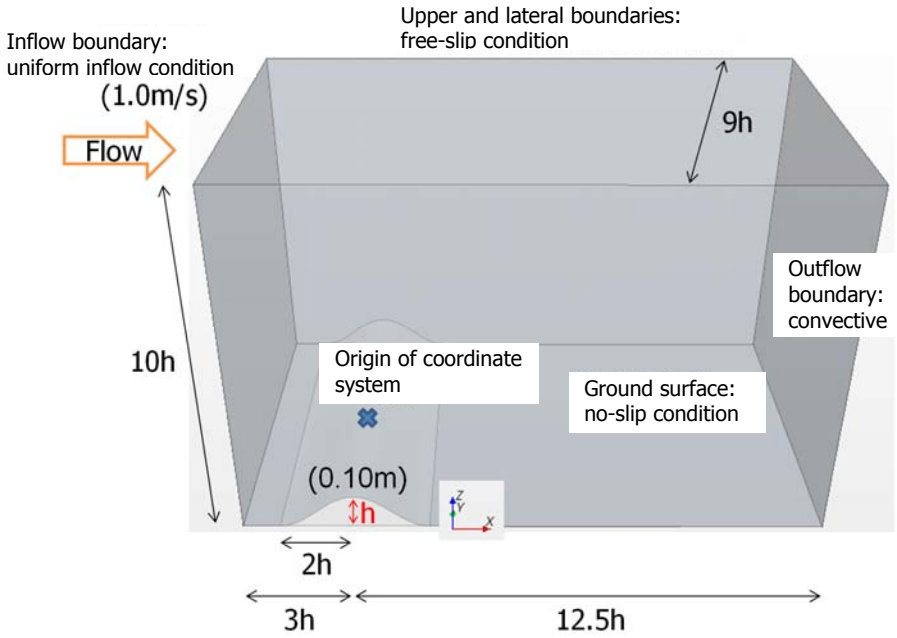

Fig.1 Computational domain, coordinate system, boundary conditions, and other related information

Poisson's equation for pressure is solved by the successive over-relaxation (SOR) method. For discretization of all the spatial terms except for the convective term in Eq.(2), a second-order central difference scheme is applied. For the convective term, a third-order upwind difference scheme is applied. An interpolation technique based on four-point differencing and four-point interpolation by Kajishima is used for the fourth-order central differencing that appears in the discretized form of the convective term. For the weighting of the numerical diffusion term in the convective term discretized by third-order upwind differencing, $\alpha = 3.0$ is commonly applied in the Kawamura-Kuwahara scheme. However, $\alpha = 0.5$ is used in the present study to minimize the influence of numerical diffusion. For LES subgrid-scale modeling, the standard Smagorinsky model is adopted with a model coefficient of 0.1 in conjunction with a wall-damping function.

5. Flow Field and Simulation-setup Considered in the Present Study

In this section, the flow field, coordinate system, and simulation-setup considered for the present study are described (Fig.1). The streamwise (x) cross-section of the ridge is identical to the central cross-section of the hill from the previous study[2].

Regarding the boundary conditions, uniform inflow conditions, free-slip conditions, and convective outflow conditions are applied at the inflow, lateral and upper, and outflow boundaries, respectively. At the ground surface, non-slip boundary conditions are imposed. The Reynolds number is set to $Re\ (= Uh / \nu) = 10^4$, where h is the ridge height and U is the wind speed at height h at the inflow boundary. The time steps are set to $\Delta t = 2 \times 10^{-3}\ (h / U)$ and $\Delta t = 2.5 \times 10^{-2}\ (h / U)$ in the simulations with RIAM-COMPACT® and STAR-CCM+, respectively.

Fig.2 shows the computational grid (structured grid) used for the simulation with RIAM-COMPACT®. The number of grid points used for this simulation is 326 (x) × 226 (y) × 67 (z) (approximately 5 million points in total). The grid points in the x- and y-directions are spaced at an even interval of 0.04h, and the grid points in the z-direction are spaced at uneven intervals ranging from 0.003h to 0.6h.

For comparison, Fig.3 shows the computational grid (unstructured grid) used for the simulation with STAR-

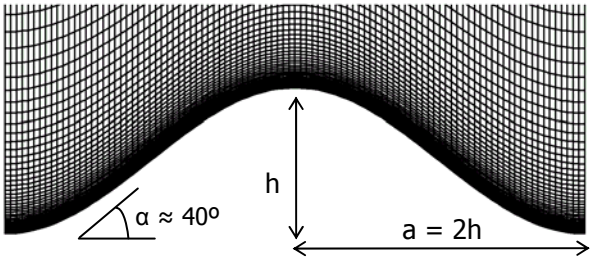

Fig.2 Computational grid in the vicinity of the ridge from the simulation with RIAM-COMPACT®, structured grid, central plane (y = 0) normal to the spanwise (y) axis

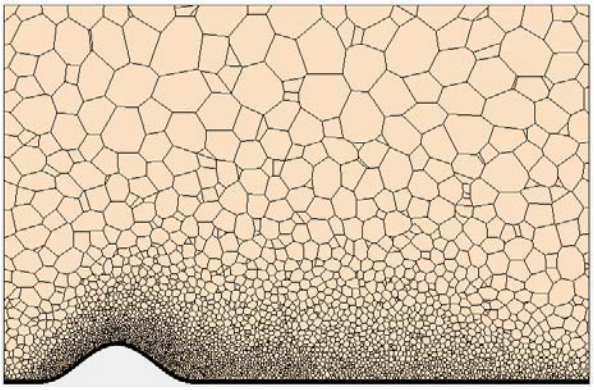

(a) Side view (y = 0), overall view

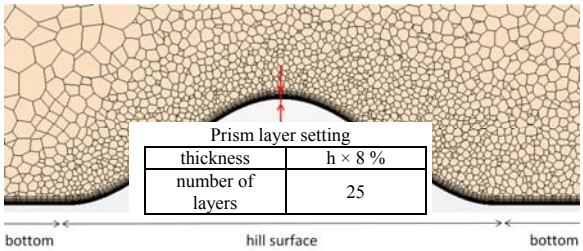

(b) Side view (y = 0), enlarged view

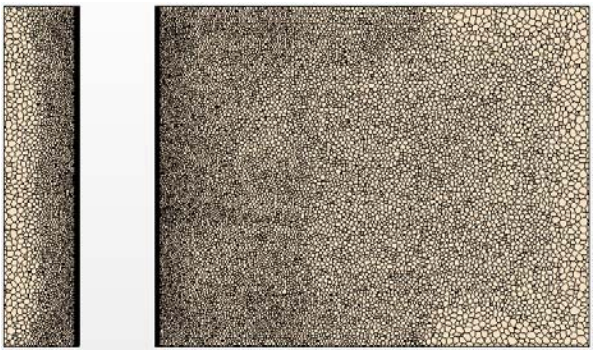

(c) Top view (z = 0.5h), overall view

Fig.3 Computational grid used for the simulation with STAR-CCM+, unstructured grid

CCM+. The total number of grid points is approximately 1.5 million (1/3 of that used for the simulation with RIAM-COMPACT®). The grid resolution in the vicinity of the ridge in the simulation with STAR-CCM+ is set to be nearly identical to that with RIAM-COMPACT®.

Tables 2 and 3 list the turbulence models (RANS and LES models) considered in the present comparative study. For convenience, simulations performed with the use of each of the models are referred to as Cases 1 to 5. The models considered in the present study are the same as those from the previous study[2]. A brief description of the WALE model used in Case 4 is as follows: the WALE model has been designed in such a way that 1) the eddy viscosity coefficient becomes zero in the vicinity of the ground surface without the use of a wall damping function and 2) the eddy viscosity coefficient is not calculated for laminar shear flow.

RANS models	**Case 1**	Spalart-Allmaras one-equation eddy-viscosity turbulence model: steady RANS
	Case 2	SST k-ω two-equation eddy -viscosity model: unsteady RANS (URANS)
LES model	**Case 3**	Standard Smagorinsky model: LES
	Case 4	WALE model: LES

Table 2 Turbulence models used in the simulations with STAR-CCM+

LES model	**Case 5**	Standard Smagorinsky model: LES

Table 3 Turbulence model used in the simulation with RIAM-COMPACT®

6. Simulation Results and Discussion

First, flow patterns generated in the vicinity of the ridge considered in the present study are described (Fig.4). The qualitative behaviors of the flows numerically simulated by RIAM-COMPACT® and observed in a wind tunnel experiment resemble each other quite closely. As was the case in the previous study[2], the shear layer which separated from the vicinity of the ridge top rolls up into isolated vortices (indicated by arrows in Fig.4 (b)). These isolated vortices then form into large-scale vortices, which are periodically shed downstream of the ridge. Refer to Uchida et al.[2] for detailed comparisons between the results of the

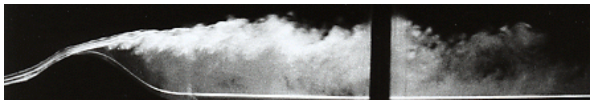

(a) Wind tunnel experiment, smoke-wire method

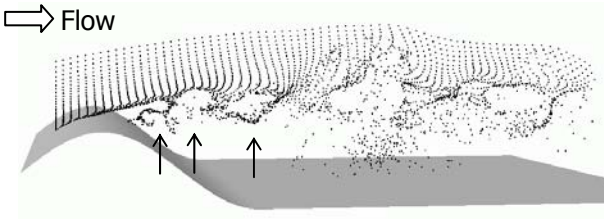

(b) Numerical simulation (RIAM-COMPACT®), passive particle tracking

Fig.4 Visualization of the flow field in the vicinity of the ridge; instantaneous field

simulation with RIAM-COMPACT® and those from the wind tunnel experiment.

Due to space limitations, Figs.5 and 6 compare the simulation results only from Case 1 (STAR-CCM+ with the steady RANS model; a steady simulation in which the steady-state solution is obtained by using the number of time steps specified in Table 1 for time marching) and Case 5 (RIAM-COMPACT® with the LES model) here as an example. Fig.7 compares the vertical profiles of the mean streamwise (x) velocity from all the cases (Cases 1 to 5). In Figs.5 to 7, the time-averaged flow field and turbulence statistics for Case 5 (RIAM-COMPACT® with the LES model) were evaluated from the time period t = 100 - 200 (h/U), An examination of Figs. 5 to 7 reveals, in contrast to the previous study[2], no significant difference between the results from the simulation which used the steady RANS model (Case 1) and those from the RIAM-COMPACT® simulation, which used the Smagorinsky LES model (Case 5), indicating that the overall trends of the flow field are similar between the two cases.

The previous study[2] investigated airflow around a three-dimensional isolated-hill, and thus, the investigated flow field was complex with the co-existence of various kinds of airflow including flow over the hill and flow around the hill. Probably because of this complex flow field, significant differences arose between the results from the simulations which used the RANS models (i.e., the steady and unsteady RANS models) and those from the simulations which used the LES models (i.e., the standard Smagorinsky and WALE models).

Since numerical simulations performed in the wind power industry are frequently for three-dimensional complex turbulent flow fields, the errors in the mean wind velocity predicted using the RANS models in the previous study[2] would greatly affect assessments of the power to be generated and other related variables. Therefore, it can be claimed that the use of the LES models is effective for simulating highly three-dimensional complex turbulent flow fields.

Although not shown here, as was the case in the previous study[2], the vertical profiles of the standard deviation of the streamwise (x) wind velocity component evaluated from the results of the simulations in the present study which used the RANS models (i.e., the steady and unsteady RANS models) showed no significant non-zero values at any position. As for the results of the simulations which used the LES models, those from STAR-CCM+ (the standard Smagorinsky and WALE models) and those from RIAM-COMPACT® (the standard Smagorinsky model) showed nearly identical trends for the vertical profiles of the standard deviation of the streamwise (x) wind velocity component (not shown).

Regarding the computational time, although the number of grid points used for the simulation with RIAM-COMPACT® (structured grid, approximately 5 million grid points) was approximately three times as large as that used for the simulations with STAR-CCM+ (unstructured grid, approximately 1.5 million grid points), the simulation with RIAM-COMPACT® completed much faster than those with STAR-CCM+, as was the case in the previous study[2].

7. Conclusion

In the previous study[2], the simulation results from RIAM-COMPACT® natural terrain version of airflow around an isolated-hill with a steep slope angle were compared to those from another commercially-available CFD software package (STAR-CCM+).

In the present paper, in order to examine the prediction accuracy of RIAM- COMPACT® (turbulence model: the standard Smagorinsky LES model), developed by the author's research group, simulations were performed with RIAM-COMPACT® and STAR-CCM+ for airflow over a ridge. The shape of the ridge is identical to the shape created by extending the central cross-section of the isolated-hill from the previous study[2] continuously in the spanwise (y) direction. The simulation results were then compared.

For the simulations with STAR-CCM+, both RANS and LES turbulence models were adopted. Specifically, for the RANS turbulence model, two such models were selected for use: the Spalart-Allmaras one-equation eddy-viscosity model (steady RANS) and the SST k-ω two-equation eddy-viscosity model (unsteady RANS). Similarly, for the LES turbulence model (SGS model), two such models were selected for use: the standard Smagorinsky model and the WALE model.

The comparisons of the simulation results revealed the following findings. The significant differences which were found for certain flow characteristics between the results of simulations with the RANS models (the steady and unsteady RANS models) and those with the LES models (the Smagorinsky and WALE models) in the previous study[2] were not found in the present study. The flow fields simulated with the use of the RANS models and those simulated with the use of the LES models showed similar overall trends.

The previous study[2] investigated airflow around a three-dimensional isolated-hill, and thus, the investigated

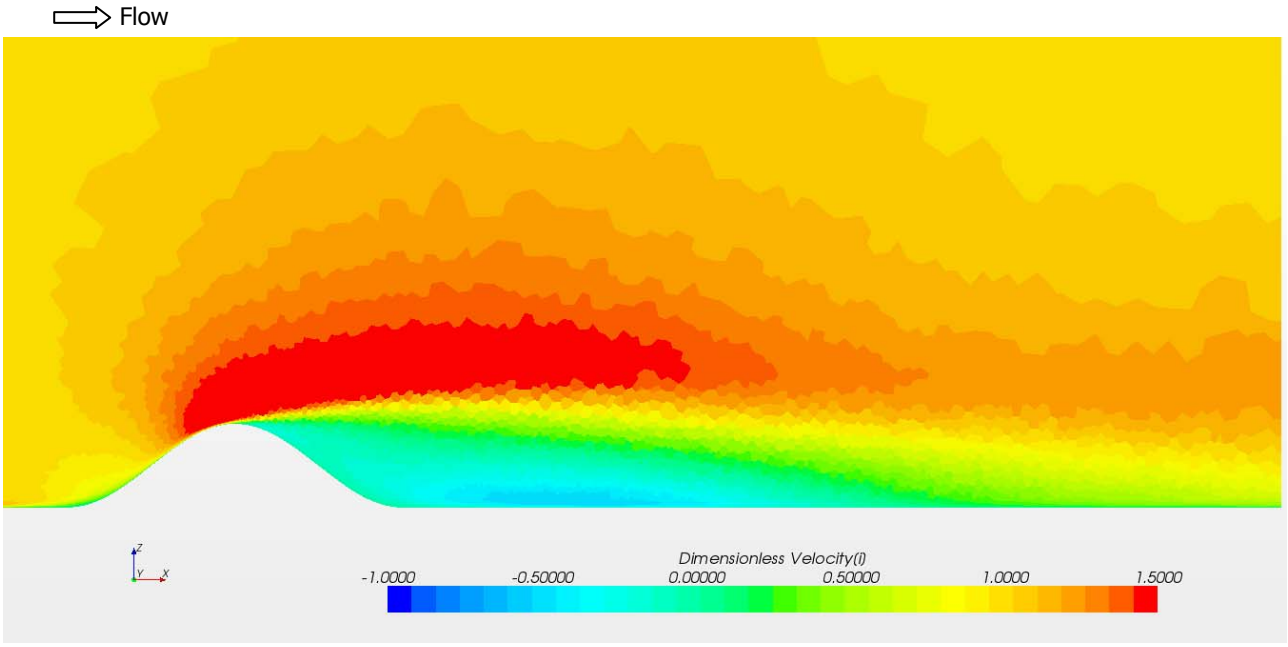

(a) Case 1, Simulation results from STAR-CCM+ with the use of the steady RANS model,
Spalart-Allmaras one-equation eddy-viscosity turbulence model

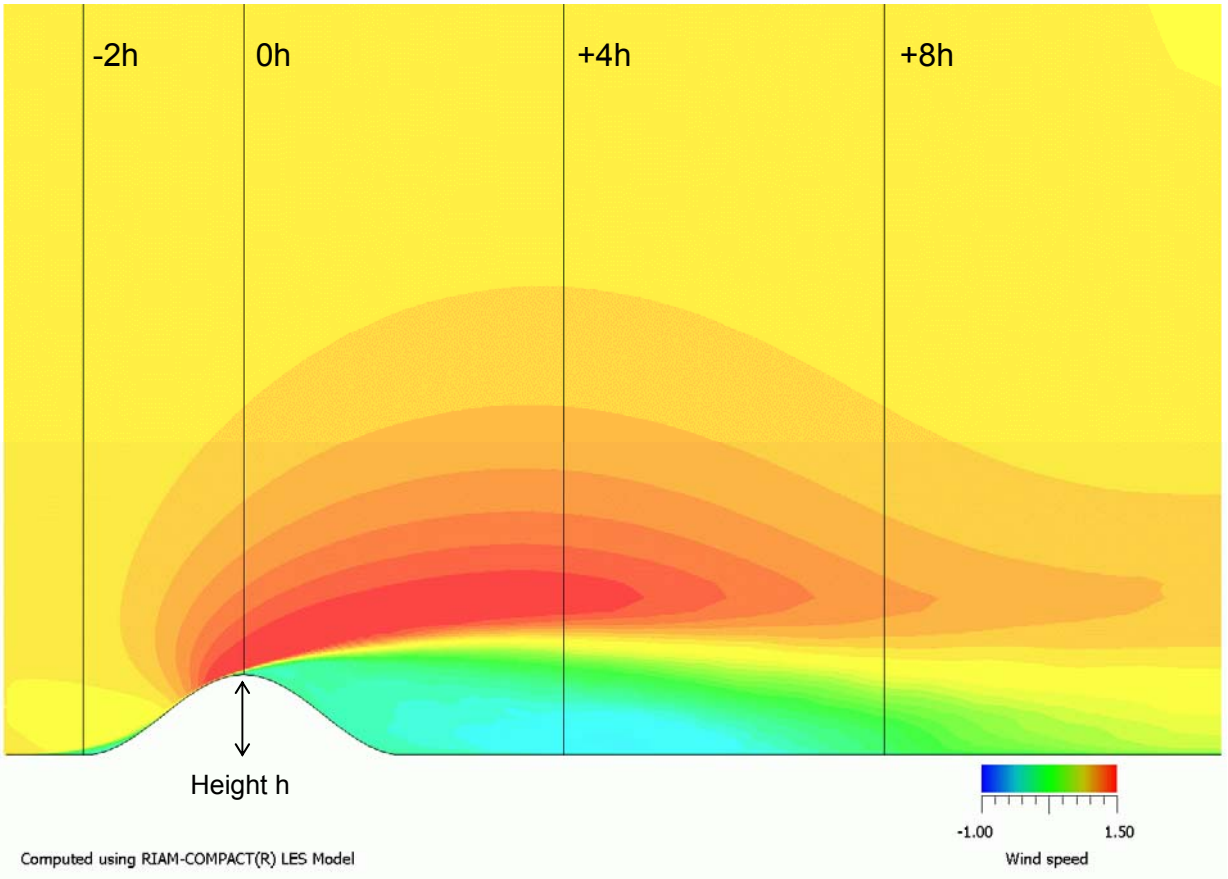

(b) Case 5, Simulation results from RIAM-COMPACT® with the use of the LES model,
the standard Smagorinsky model, time-averaged field

Fig.5 Comparison of the streamwise (x) velocity component distribution,
central plane (y = 0) normal to the spanwise (y) axis.
Here, the velocity component is normalized by the magnitude of the uniform inflow wind velocity.

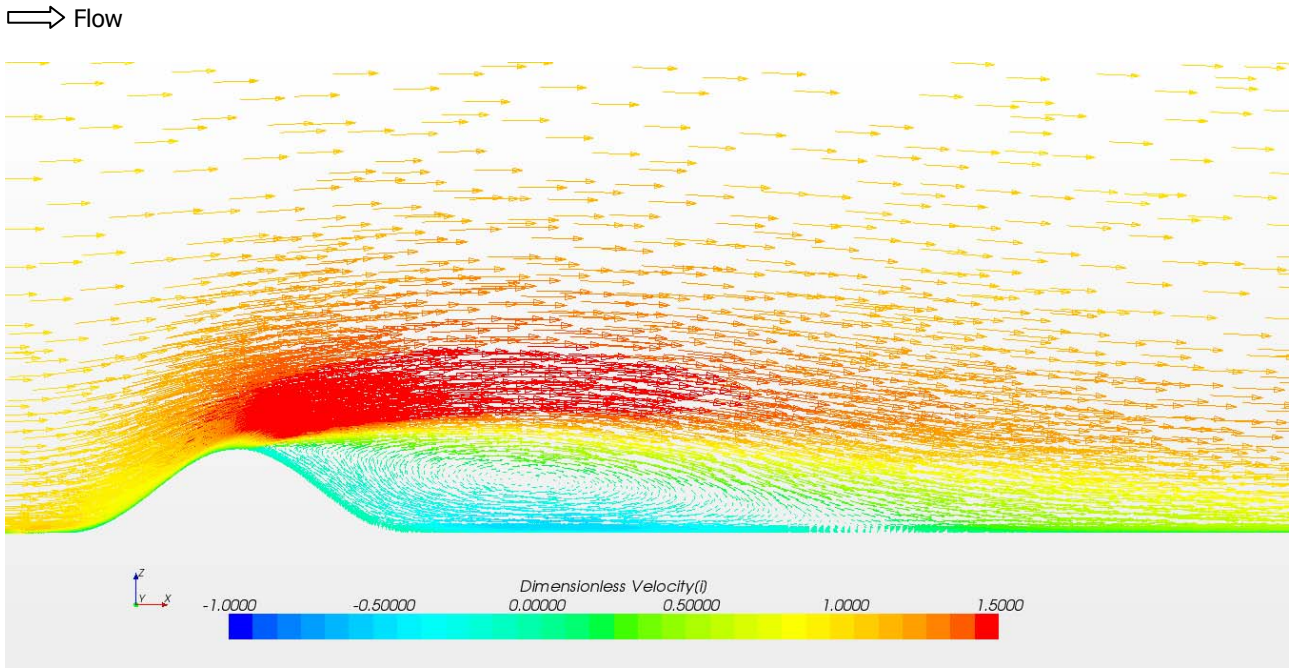

(a) Case 1, Simulation results from STAR-CCM+ with the use of the steady RANS model, Spalart-Allmaras one-equation eddy-viscosity turbulence model

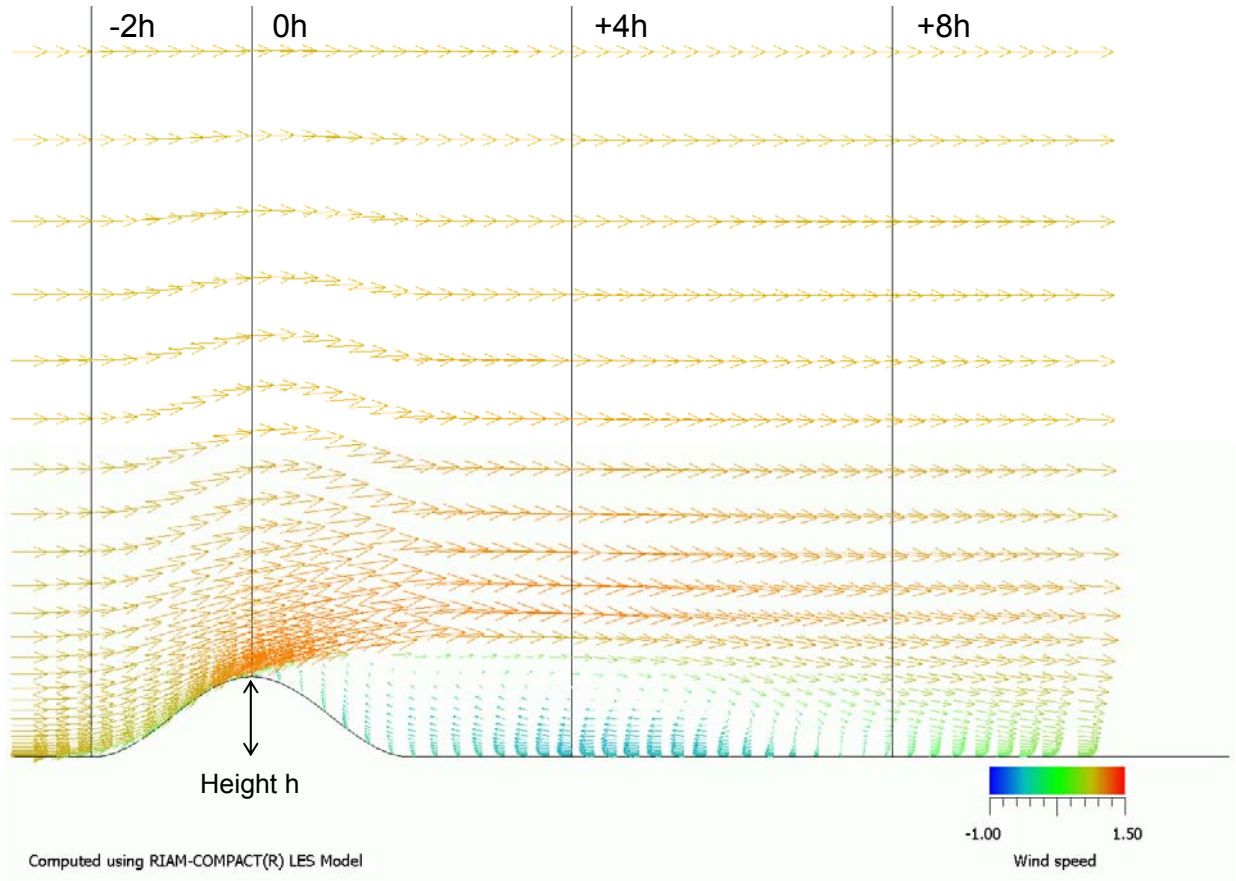

(b) Case 5, Smulation results from RIAM-COMPACT® with the use of the LES model, the standard Smagorinsky model, time-averaged field

Fig. 6 Comparison of velocity vectors, central plane (y = 0) normal to the spanwise (y) axis. Here, the velocity components are normalized by the magnitude of the uniform inflow wind velocity.

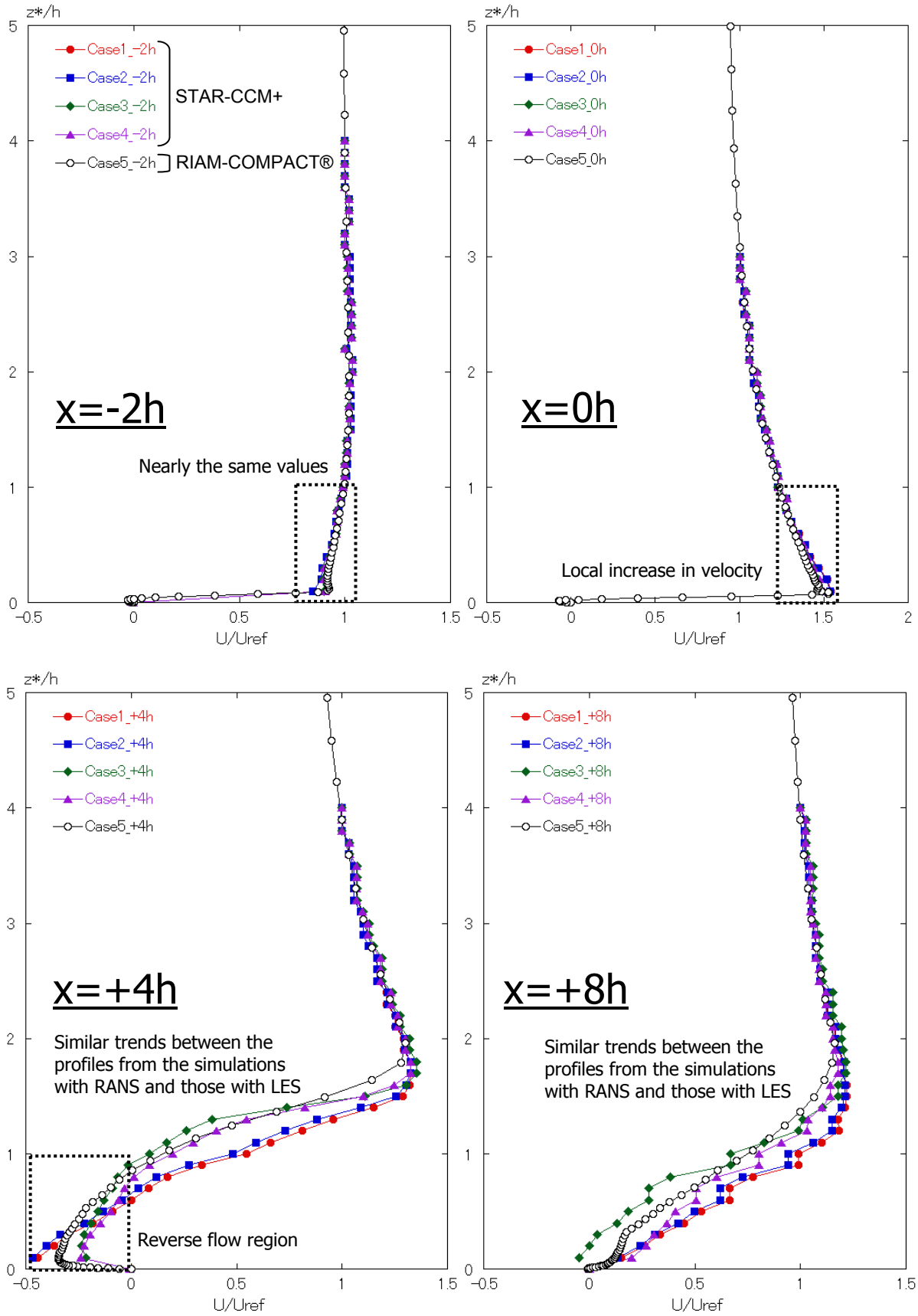

Fig. 7 Comparison of the mean streamwise (x) velocity profiles. Here, the velocity component is normalized by the mean upper-air streamwise (x) velocity above the location of each profile evaluation.

flow field was a complex turbulent flow field with the co-existence of various kinds of airflow including flow over the hill and flow around the hill. Probably for this reason, significant differences arose between the results from the simulations which used the RANS models and the results from the simulations which used the LES models in the previous study[2]. Since numerical simulations in the wind power industry are frequently performed for three-dimensional, complex turbulent flow fields, the errors in the mean wind velocity predicted using the RANS models in the previous study[2] would greatly affect assessments of the power to be generated and other related variables. Therefore, it can be claimed that the use of the LES models is effective for simulating highly three-dimensional complex turbulent flow fields.

As was the case in the previous study[2], the vertical profiles of the standard deviation of the streamwise (x) wind velocity component evaluated from the simulations which used the RANS models (i.e., the steady and unsteady RANS models) showed no significant non-zero values at any position in the present study. As for the results of the simulations which used the LES models, the trends of this variable from STAR-CCM+ (the standard Smagorinsky and WALE models) and those from RIAM-COMPACT® (the standard Smagorinsky model) were nearly identical.

Regarding the computational time, although the number of grid points used for the simulation with RIAM-COMPACT® was approximately three times as large (structured grid, approximately 5 million grid points) as that used for the simulations with STAR-CCM+ (unstructured grid, approximately 1.5 million grid points), the simulation with RIAM-COMPACT® completed much faster than those with STAR-CCM+, as was the case in the previous study[2].

References

1) Takanori UCHIDA, Validation Testing of the Prediction Accuracy of the Numerical Wind Synopsis Prediction Technique RIAM-COMPACT for the Case of the Bolund Experiment –Comparison against a Wind-Tunnel Experiment–, Reports of RIAM, Kyushu University, No.147, pp.7-14, 2014

2) Takanori UCHIDA, Reproducibility of Complex Turbulent Flow Using Commercially-Available CFD Software –Report 1: For the Case of a Three-Dimensional Isolated-Hill With Steep Slopes–, Reports of RIAM, Kyushu University, No.150, in press, 2016

Appendix

In this appendix, comparisons are made between the results of the simulation with RIAM-COMPACT® (turbulence model: the standard Smagorinsky LES model) from the present study and those from the wind tunnel experiment performed by the author previously. In both Figs.8 and 9, the variables on the horizontal and vertical axes are normalized by the mean upper-air streamwise (x) velocity, U_{ref}, above the location of each profile evaluation and the height of the ridge, h, respectively. The variable z* on the vertical axis represents the height above the flat surface.

The simulations in the present study are performed for airflow over a ridge, the shape of which is identical to the shape created by extending the central cross-section of the isolated-hill from the previous study[2] continuously in the spanwise (y) direction. Therefore, both the simulation and wind tunnel results are more subject to the effect of the blockage ratio than those in the previous study. Specifically, at the ridge top (Fig.8(b)), the wind speed-up ratio for the simulation is significantly overestimated with respect to that for the wind tunnel. As a result, differences in the flow field arise between the two results, including a difference in the size of the vortex region downstream of the ridge (Figs.8(c), 8(d), 9(c), and 9(d)). Although the above-mentioned differences in the flow fields exist, the overall trends of the flow fields are in agreement between the simulated and wind-tunnel flows in Figs.8 and 9.

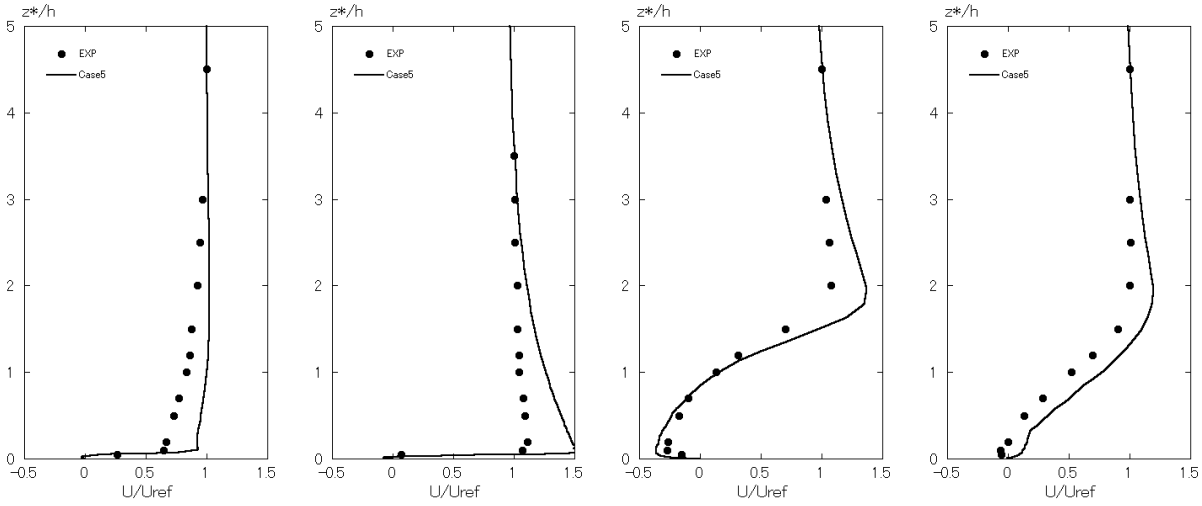

Fig.8 Comparison of the mean streamwise (x) velocity profiles,
filled circle: wind tunnel experiment, line: simulation with RIAM-COMPACT® (turbulence model: LES)

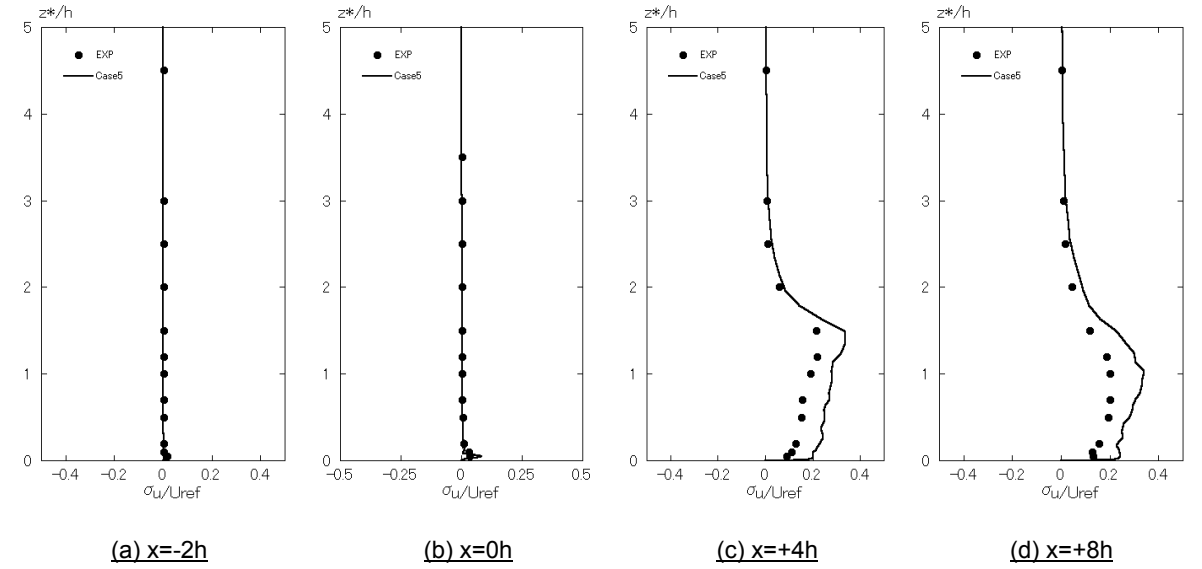

Fig.9 Comparison of the standard deviation of the streamwise (x) velocity,
filled circle: wind tunnel experiment, line: simulation with RIAM-COMPACT® (turbulence model: LES)